Iranian Journal of Medical Physics

ijmp.mums.ac.ir

Investigation of Neutron Contamination of Flattening Filter and Flattening Filter-Free 10-MV Photon Beams in Elekta Infinity™ Accelerator

Sitti Yani[1,2*], Indra Budiansah[2], Fauzia Puspa Lestari[2], Rasito Tursinah[3], Mohamad Fahdillah Rhani[4], Freddy Haryanto[2]

1. Bogor Agricultural University (IPB University), Bogor, Indonesia
2. Institut Technologi Bandung, Bandung, Indonesia
3. National Nuclear Energy Agency, Bandung, Indonesia
4. Concord International Hospital, Singapore

ARTICLE INFO

Article type:
Original Article

Article history:
Received: Jan 25, 2019
Accepted: Jul 05, 2019

Keywords:
Neutron
Monte Carlo Method
Photon Beam
Linear Accelerator

ABSTRACT

Introduction: This study aimed to measure the neutron contamination of flattening filter (FF) and flattening filter-free (FFF) 10-MV photon beams delivered by the Elekta Infinity™ accelerator.

Material and Methods: The photoneutron spectrum produced by the Linac head was evaluated using a Monte Carlo (MC) simulation. The geometry and composition of the head Linac material were modelled based on information obtained from the manufacturer. In this simulation, MC N-Particle Transport Code software (MCNP6) was utilized to model the Linac head and simulate the particle transport. Evaluation of neutron contamination was carried out for the Linac with FF and without it (i.e., FFF). In this regard, the FFF beam was built by removing the FF from the Linac components. The scoring plane, as the neutron spectra calculation area for FF and FFF beams, was placed 99 cm from the target.

Results: The neutron type produced by the head Linac Elekta Infinity™ 10-MV photon mode was mostly thermal and fast. Although there were differences in the neutron intensity of FF and FFF beams, the type of neutrons produced by these two modes had the same energy. Based on the photoneutron reaction energy threshold, it can be concluded that the neutrons produced from the head Linac were the result of photoneutron interactions of high-energy photons with molybdenum-96 and tungsten-184 isotopes.

Conclusion: The photoneutron quantity did not change for FF and FFF beams; however, a larger quantity of neutrons was produced in the FF beam.

► *Please cite this article as:*
Yani S, Budiansah I, Lestari FP, Tursinah R, Rhani MF, Haryanto F. Investigation of Neutron Contamination of Flattening Filter and Flattening Filter-Free 10-MV Photon Beams in Elekta Infinity™ Accelerator. Iran J Med Phys 2020; 17: 126-132. 10.22038/ijmp.2019.37195.1471.

Introduction

Linear accelerator (Linac) operating above 8 MV produces photoneutrons whether it operates in the electron or X-ray mode. Particle contaminations, neutrons, and electrons are created through the interaction between bremsstrahlung photons and Linac components [1-6]. Neutrons have high radiobiological effectiveness, compared with photons and electrons, regarding the dose deposited in the tissue. Accordingly, these photoneutrons can scatter throughout the treatment room, reach the patient body, and induce harmful effects.

Hashemi et al. (2007) investigated the photoneutron spectrum produced by an 18-MV Saturne Linac at different points of a treatment room. They found that fast neutrons rapidly decreased due to distance enhancement from the beam center. However, the number of thermal neutrons did not significantly change [7]. Neutron spectra measurements by Howell et al. (2009) showed that the neutron fluence was at the highest rate for the 18-MV Varian 21EX beam, which was 2.9 times greater than that of the Elekta Linac [8].

The neutron source strength of various Linacs was different, depending on the photon energy, Linac head structures, and a model based on some studies reviewed by Naseri and Mesbahi (2010) [9]. Elekta SL-20 and SL-25 18-MV photon beams produced a neutron strength of about 0.46×10^{12} [10]. To the best of our knowledge, photoneutron of new Elekta series, Elekta Infinity™ 10-MV photon beam Linac, has never been studied before.

The main components in the Linac head which produce photoneutrons are flattening filter (FF), primary collimator, multileaf collimator (MLC), and jaws. The current research was mostly directed at removing FF from Linac models, referred to as flattening filter-free (FFF) [11-15]. One of the objectives of FFF is to reduce the number of particle

*Corresponding Author: Tel: +62-813-1334-9960; Email: sitti.yani@s.itb.ac.id

contaminant, including photoneutron produced by Linac [16]. Some studies have been conducted to investigate the effect of FFF on the number of contaminant particle, surface dose, and other factors in radiotherapy [17-20]. The measurement, analytical, and Monte Carlo (MC) method can be used to measure neutron contamination in Linac.

Monte Carlo methods are highly accurate but expensive (in terms of calculation time). Monte Carlo N-Particle Transport Code software (MCNP) is a general-purpose code that can simulate particle transport. The MC method is an efficient tool to be used in processes that have erratic behaviours, such as high-energy physics, particle transport, financial analysis, and process engineering. Several MC simulation programs have been utilized to determine the dose distribution in homogenous/inhomogeneous phantom and particle contaminant of Linac [4-6, 21-29].

Particle contamination in medical Linac has been investigated by many authors using the MC method. In this regard, Medina et al. (2005) and Allahverdi et al. (2011) characterized electron contamination in photon beams by applying the MC method. They found that the amount of electron contamination was increased by the rise of the Linac energy. The FF and the beam monitor chamber located in the central axis are the primary sources of electron contamination [30, 31]. Our previous studies (Yani et al.; 2016 and 2017) demonstrated the same results for Varian Clinac iX 6 and 10-MV photon beam, using the EGSnrc MC package. The neutron contamination energy of Varian Clinac iX 10 MV at a source to surface distance (SSD) of 100 cm was a fast neutron (2.239 MeV) [5, 23]. The produced photoneutrons can result in unwanted dose to not only the patient inside the treatment room but also the general public and radiation workers outside the treatment room.

Therefore, the aim of this study was to measure the amount of neutron contamination of 10 MV-FF and FFF photon beams delivered by the Elekta Infinity™ head Linac (Elekta AB, Stockholm, Sweden).

Materials and Methods

The X-ray beam produced from 10 MV FF and FFF Elekta Infinity™ photon beams was simulated by transporting a mono-energetic electron beam, using MCNP6 user codes developed by Los Alamos National Laboratory (LANL). A two-dimensional (Y, Z) representation of the Linac model was adopted from the manufacturer. The neutron contamination was scored at a distance of 99 cm from the target (scoring plane).

MCNP6

Monte Carlo methods are highly accurate but expensive (in terms of calculation time). A general-purpose Monte Carlo N-Particle, version 6 (MCNP6) can simulate transport particles in complex geometry and cannot be modeled with analytical and deterministic methods. The code deals with the transport of particles (e.g., neutrons, photons, electrons, combined neutrons and photons, combined neutrons, photons and electrons, or combined photons and electrons). This code can be used to simulate such domains as radiation shielding, accelerator target design, dosimetry, radiotherapy, radiodiagnososis, and reactor design. This code was developed at the Los Alamos National Laboratory (LANL) [32].

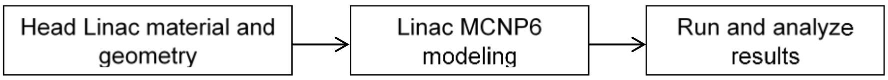

Figure 1. Simulation steps adopted in this study

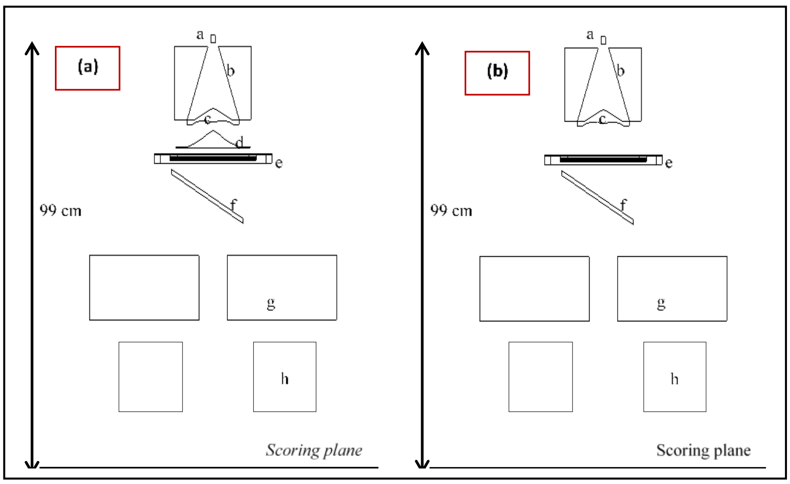

Figure 2. Schematic diagrams of (a) 10-MV FF and (b) FFF Elekta Infinity™

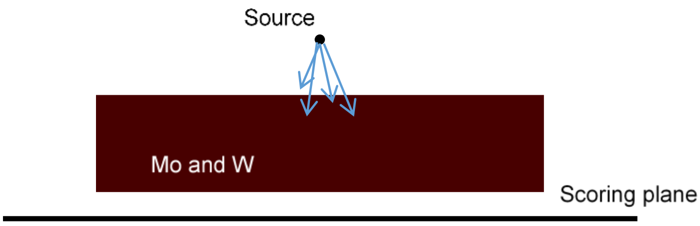

Figure 3. Simple geometry of molybdenum and tungsten slab simulation

Table 1. Components and materials in Linac head

	Components	Materials	Distance from the target (cm)
a	Target	$_{74}W$, $_{75}Re$	0
b	Primary collimator	$_{74}W$, $_{26}Fe$, $_{28}Ni$	1.66
c	Difference filter	Stainless steel Bar BS EN 1008-3 X8CrNiS 18-9	8.70
d	Flattening filter	$_{26}Fe$, $_{24}Cr$, $_{28}Ni$, $_{25}Mn$, $_{42}Mo$, $_{14}Si$, $_{16}S$, $_{6}C$, $_{15}P$	13.30
e	Ion chamber	$_{6}C$, $_{1}H$, $_{8}O$	16.44
f	Mirror	$_{13}Al$	18.54
g	Jaws	$_{74}W$, $_{26}Fe$, $_{28}Ni$	34.93
h	Multileaf collimator	$_{74}W$, $_{26}Fe$, $_{28}Ni$	39.45
	Scoring plane	$_{6}C$, $_{7}N$, $_{8}O$, $_{18}Ar$	99.00

Linac head modeling

The simulated Linac model includes the target, primary collimator, difference filter, FF, ion chamber, mirror, MLC, and jaws with material compositions presented in Table 1. The electron and photon cut-off energies were set at 0.7 and 0.01 MeV, respectively. No variance reduction technique was applied in this simulation. The incident particle was electron with an energy of 10.5 MeV and to z-direction point source. The electrons hit the target to produce the bremsstrahlung photon. The FF and FFF Linacs were modeled using MCNP6. The FF was removed from the Linac model to simulate 10 MV-FFF Linac (Figure 2). The field size was set at 10×10 cm^2 using MLC. The material data were provided by LANL with respect to photoneutron interaction.

The F4 tally was used to calculate the photon, electron, and neutron fluence profiles, energy spectra, and mean energy profiles at the scoring plane (SSD=99 cm). The scoring plane material was filled with air with dimension 25×25×1 cm^3. Totally, 2×10^9 electron histories were simulated. Air material at a density of 0.00012 g/cm^3 filled the surrounding Linac model with non-zero importance (IMP: E 1, IMP: P 1, and IMP: N 1). The maximum statistical uncertainty of the results at the scoring plane for several cases was about 2%. The used Central Processing Unit (CPU) for the simulation was an Intel Pentium core i5 with 3-GHz processors. By reading the output data from the scoring plane, the energy spectra can be analyzed.

Photon and neutron fluence after Mo and W slabs

This step was taken to investigate the Linac constituent materials that contribute to neutron production. The molybdenum ($_{42}Mo$) and tungsten ($_{72}W$) were chosen to this end. The Mo and W slab with varied thicknesses of 0.5, 1.0, 1.5, 2.0, and 2.5 cm were hit by an incidence of 10.5 MeV electron. The produced particles due to the interaction of electron with Mo and W materials were scored at a distance of 3.0 cm from the source position (Figure 3). This simulation was performed using the same CPU as the previous case. The statistical uncertainty of the results at their scoring plane was <1%.

Results

Photon and neutron trajectories

Figure 4 shows the trajectories of the 1.5-MeV photon, 0.08-MeV neutron, and 1.5-MeV neutron in a water phantom. These figures were obtained from the Geant4-Gamos with 100 histories (http://fismed.ciemat.es/GAMOS/). For the same energy (1.5 MeV), the photon track was more than neutrons.

Neutron fluence in scoring plane

Figure 5 depicts the neutron fluence in the scoring plane (99 cm from target). The total intensity of the neutron Linac with FF was almost two times larger, compared to that of the FFF beam. The total intensities of Linac FF and FFF were 1.52×10^{-9} and 2.55×10^{-9} cm^{-2}, respectively. However, even though the FF was removed, the produced neutron energy did not change (319 keV for FF and 312 keV for FFF).

Photon and neutron fluence after Mo and W slabs

Figure 6 illustrates the intensity of photon produced from the electron beam hitting Mo and W targets. The photon intensity in the scoring plane for Mo was 2-fold higher than that in W target.

The total intensities of photo-neutron produced below the W target were 3.73×10^{-9}, 4.84×10^{-9}, 5.02×10^{-9}, 4.86×10^{-9}, and 5.09×10^{-9} cm^{-2} for 0.5, 1.0, 1.5, 2.0, and 2.5 cm W thickness, respectively. The maximum energy of photoneutron produced was 1.26 MeV. However, Mo did not produce photoneutron at all in this case.

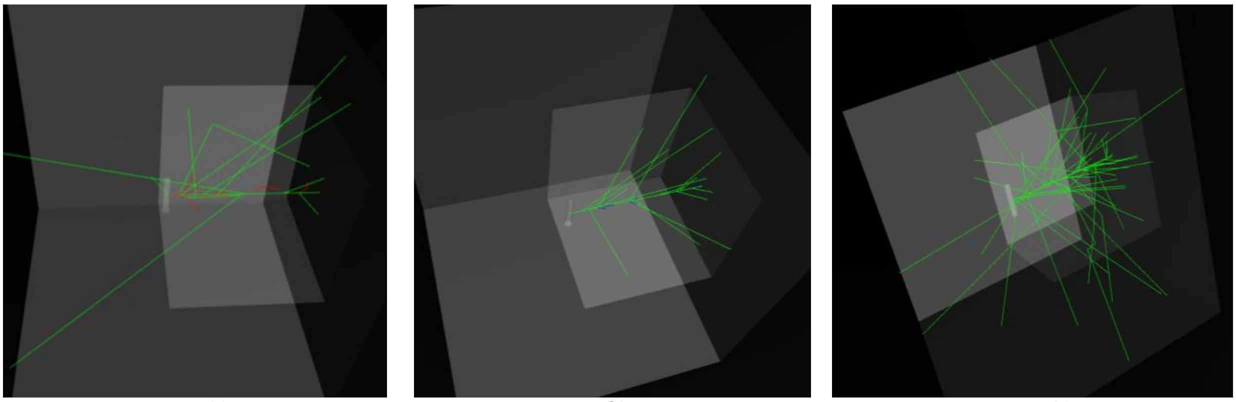

(a) (b) (c)

Figure 4. a) Photon trajectories (E=1.5 MeV), b) neutron trajectories (E=0.08 MeV), and c) neutron trajectories (E=1.5 MeV) using Gamos/Geant4

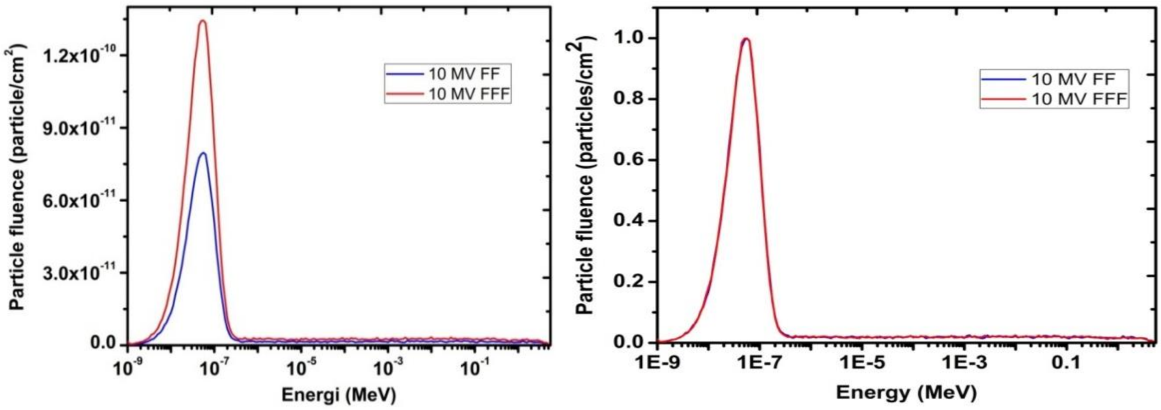

Figure 5. Neutron fluence of 10-MV FF and FFF Elekta Infinity^{TM} 10-MV photon beams (a) before and (b) after normalization

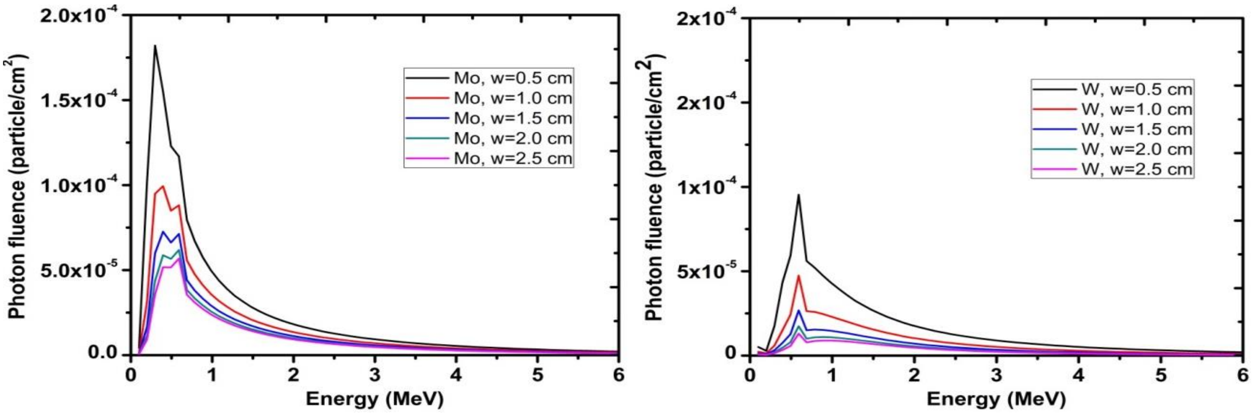

Figure 6. Photon fluence of the scoring plane (2.5 cm from the target)

Discussion

Photons in Linac head are produced when high-energy electrons collide with a high atomic number target, such as W and rhenium slab. The maximum energy of the produced X-ray spectrum was equal to the incident electron energy. When X-rays with the energies of > 7 MeV collide with high atomic number materials that are found in the target, primary collimator, difference filter, FF, ion chamber, MLC or jaws, they can generate neutrons. These neutrons came from X-ray interaction with high atomic number (Z) nuclei and are known as photoneutrons. The neutron production is based on the following equation:

$$\gamma + {}^{184}_{74}W \rightarrow {}^{183}_{74}W + n \quad (1)$$

The neutrons have a wide range of energies from 0.025 eV to 10 MeV. The neutrons with the energies of < 0.025 eV, 0.025 eV-1 keV, 1 keV-0.5 MeV, 0.5-10 MeV, and >10 MeV were called thermal, slow, resonance, fast, and high-energy neutron, respectively. These neutrons can scatter in all directions in the treatment room. Radiation protection calculations for photoneutrons generated from Linac are aimed to protect both patients and staff from the unwanted radiation.

The Gamos-Geant4 was used to simulate the photon and neutron trajectories in water phantom (Figure 5). As with photons, the higher the energy is, the more extended the particle travels. Neutrons have longer tracks than photons in water, even though they have the same energy. The 1.5-MeV photon can produce the secondary particles in the form of electron and positron (red and blue lines in Figure 4(a). Secondary particles were not generated in 1.5-MeV neutron.

Figure 5 displays that the removal of FF did not affect the neutron contamination energy. Photoneutron mean energy only changes around 7 keV for FFF than for FF beam. The mean energy of photoneutrons was measured at 319 and 312 keV for FF and FFF beams, respectively. Thermal neutrons can be produced from elastic and inelastic collisions in the Linac head. These neutrons significantly contribute to patient effective dose and can be harmful to the patient [33].

The neutron contamination fluence found in this study was compared to our previous results about neutron produced in the Varian Clinac iX 10-MV photon beam [4]. In this study, mean neutron energy was lower than the neutron produced by Varian and affected the effective dose. The mean photoneutron energies in the scoring plane were 0.319 and 2.239 MeV for 10-MV Elekta Infinity™ and 10-MV Varian Clinac iX photon beams, respectively. The difference in mean energy was more than 100%. This lower mean energy was caused by several factors, including the primary collimator and MLC of the Varian, which were thicker than the one in the Elekta.

Copper FF was located in the beam axis, and Varian has two pairs of jaws, namely jaws X and jaws Y, that made from W material. Mesbahi and Naseri (2010) found that the neutron strength for the Varian was more significant than for the Elekta with an energy of 18 MV. The thermal neutron was produced in the treatment room in Linac Siemens, Varian, and Elekta [9]. Thermal neutrons in this study were also presented in a study conducted by Followill et al. (2003) [10]. The produced neutron energy is lower than the neutrons produced by Elekta SL-20 and SL-25 due to different Linac energy.

Simple geometry was simulated to investigate the effect of the material inside the Linac on photoneutron production. The Mo and W slabs with varied thicknesses were used, and photon and neutron fluence was collected after this geometry. The 10.5-MeV electron hitting slab can produce photoneutron in W material; however, no photoneutron was genereated in Mo material. The bremsstrahlung photon was formed in all slab simulated (Figure 6). It can be inferred from the figure that the thicker the material, the lower the number of photons recorded in the scoring plane for both W and Mo materials. Tungsten which is denser than Mo causes fewer photon fluence. The photon mean energy in W was higher than in Mo.

The total intensity of photoneutron of W slab depends on the material thickness. These neutrons are fast neutrons that can travel a longer distance than thermal neutrons. Consequently, they are dangerous not only for patients but also for radiation workers. The mean energy of the produced photoneutron was 0.334 MeV for all thicknesses.

From the obtained results, it can be said that W has a greater chance than Mo in producing neutrons in the Elekta Infinity™ Linac. In addition to the composition of the material inside the beam, it is more dominated by W. Furthermore, W had smaller threshold energy than Mo in producing photoneutrons.

Conclusion

This study showed that thermal neutron contamination was produced in FF and FFF head Linac Elekta Infinity™ 10-MV photon beams. The photoneutron quantity in the scoring plane (99 cm from target) was not changed for FF and FFF; however, a larger neutron quantity was produced in the FFF beam. The contaminant source might emanate from the interaction of bremsstrahlung photon with the target, primary collimator, FF, or MLC. Future research will be directed at the calculation of neutron strength and the equivalent dose of photoneutrons produced by Elekta Infinity™ 10-MV photon beams.

Acknowledgment

Authors would like to thank Insentif In House Post-Doctoral 2018, Institut Teknologi Bandung, and World Class University, Indonesia.

References

1. Alem-Bezoubiri A, Bezoubiri F, Badreddine A, Mazrou H, Lounis-Mokrani Z. Monte Carlo estimation of photoneutrons spectra and dose equivalent around an 18 MV medical linear

accelerator. Radiation Physics and Chemistry. 2014; 97:381‐92.
2. Mohammadi A, Afarideh H, Davani FA, Ghergherehchi M, Arbabi A. Monte Carlo study of neutron-ambient dose equivalent to patient in treatment room. Applied Radiation and Isotopes. 2016; 118: 140‐8.
3. Yucel H, Cobanbas I, Kolbas A, Yuksel AO, Kaya V. Measurement of photo-neutron dose from an 18-MV medical linac using a foil activation method in view of radiation protection of patients. Nuclear Engineering and Technology. 2016; 48:525‐32.
4. Yani S, Tursinah R, Rhani MF, Soh RCX, Haryanto F, Arif I. Neutron contamination of Varian Clinac iX 10 MV photon beam using Monte Carlo simulation. Journal of Physics: Conference Series. 2016; 694:012020.
5. Yani S, Dirgayussa IGE, Rhani MF, Soh RCX, Haryanto F, Arif I. Monte Carlo study on electron contamination and output factors of small field dosimetry in 6 MV photon beam. Smart Science. 2016; 4(2):87-94.
6. Abou-Taleb WM, Hassan MH, El-Mallah EA, Kotb SM. MCNP5 evaluation of photoneutron production from the Alexandria University 15 MV Elekta Precise medical Linac. Applied Radiation and Isotopes. 2018; 135:184‐91.
7. Hashemi SM, Hashemi-Malayeri B, Raisali G, Shokrani P, Sharafi AA. A study of the photoneutron dose equivalent resulting from a Saturne 20 medical linac using Monte Carlo method. Nukleonika. 2007; 52(1):39–43.
8. Howell RM, Kry SF, Burgett E, Hertel NE, Followill DS. Secondary neutron spectra from modern Varian, Siemens, and Elekta linacs with multileaf collimators. Med. Phys. 2009; 36(9):4027- 38.
9. Naseri A, Mesbahi A. A review on photoneutrons characteristics in radiation therapy with high-energy photon beams. Reports of Practical Oncology and Radiotherapy. 2010; 15:138‐44.
10. Followill DS, Stovall MS, Kry SF, Ibbott GS. Neutron source strength measurements for Varian, Siemens, Elekta, and General Electric linear accelerators. J Appl Clin Med Phys. 2003; 4:189‐94.
11. Mesbahi A. Dosimetric characteristics of unflattened 6 MV photon beams of a clinical linear accelerator: a Monte Carlo study. Applied Radiation and Isotopes. 2007; 65:1029‐36.
12. Kragl G, af Wetterstedt S, Knäusl B, Lind M, McCavana P, Knöös T, et al. Dosimetric characteristics of 6 and 10MV unflattened photon beams. Radiother Oncol. 2009; 93(1):141-6.
13. Jank J, Kragl’ G, Georg D. Impact of a flattening filter free linear accelerator on structural shielding design. Z. Med. Phys. 2014; 24:38‐48.
14. Ashokkumar S, Nambira A, Sinha S N, Yadava G, Ramana K, Bhushana M, et al. Measurement and comparison of head scatter factor for 7 MV unflattened (FFF) and 6 MV flattened photon beam using indigenously designed columnar mini phantom. Reports of Practical Oncology and Radiotherapy. 2015; 20:170‐80.
15. Chung JB, Kim JS, Eom KY, Kim IA, Kang SW, Lee JW, et al. Comparison of VMAT-SABR treatment plans with flattening flter (FF) and flattening flter-free (FFF) beam for localized prostate cancer. Journal of Applied Clinical Medical Physics. 2015; 16(6):302‐13.
16. Kry SF, Titt U, Ponisch F, Vassiliev ON, Salehpour M, Gillin M, et al. Energy spectra, sources, and shielding considerations for neutrons generated by a flattening filter-free Clinac. International Journal of Radiation Oncology, Biology, and Physics. 2007; 68:1260‐4.
17. Pichandi A, Ganesh KM, Jerin A, Balaji K, Kilara G. Analysis of physical parameters and determination of inflection point for Flattening Filter Free beams in medical linear accelerator. Reports of Practical Oncology and Radiotherapy. 2014; 19:322‐31.
18. Mesbahi, A. Dosimetric characteristics of unflattened 6 MV photon beams of a clinical linear accelerator: A Monte Carlo study. Applied Radiation and Isotopes. 2007;65:1029‐36.
19. Najem MA, Spyrou NM, Podolyák Z, Abolaban FA. The physical characteristics of the 15 MV Varian Clinac 2100C unflattened beam. Radiation Physics and Chemistry. 2014; 95:205‐9.
20. Wang Y, Khan MK, Ting JY, Easterling SB. Surface Dose Investigation of the Flattening Filter-Free Photon Beams. Int J Radiation Oncol Biol Phys. 2012; 83(2):281-5.
21. Ezzati AO, Mahdavi SR, Anijdan HM. Size Effects of Gold and Iron Nanoparticles on Radiation Dose Enhancement in Brachytherapy and Teletherapy: A Monte Carlo Study. Iranian Journal of Medical Physics. 2013; 11(2&3):253-9.
22. Tartar A. Monte Carlo simulation approaches to dose distributions for 6 MV photon beams in clinical linear accelerator. Biocybernetics and Biomedical Engineering. 2014; 34:90‐100.
23. Yani S, Rhani MF, Soh RCX, Haryanto F, Arif I. Monte Carlo simulation of varian clinac iX 10 MV photon beam for small field dosimetry. International Journal of Radiation Research. 2017; 15(3):275-82.
24. Ghavami SM, Ghiasi H. Estimation of Secondary Skin Cancer Risk Due To Electron Contamination in 18-MV LINAC-Based Prostate Radiotherapy. Iranian Journal of Medical Physics. 2016; 13(4):236-49.
25. Zolfaghari M, Sedaghatizadeh M. Design and Simulation of Photoneutron Source by MCNPX Monte Carlo Code for Boron Neutron Capture Therapy. Iranian Journal of Medical Physics. 2015; 12(2):129-36.
26. Sadoughi HR, Nasseri S, Momennezhad M, Sadoghi-Yazdi H, Zare MH, Bahreyni-Toosi MH. Calculations of Linac Photon Dose Distributions in Homogeneous Phantom Using Spline. Iranian Journal of Medical Physics. 2013; 10(3):133-8.
27. Aghaebrahimian A, Alamatsaz MH. Monte Carlo Evaluation of Gamma Knife Dose Profile in Real Brain Phantom. Iranian Journal of Medical Physics. 2016; 13(1):1-7.
28. Horová S, Judas L. Monte Carlo modelling of clinical accelerator beams and estimation of primary electron beam parameters. Radioprotection. 2018; 53(1):61‐6.
29. Yani S, Tursinah R, Rhani MF, Haryanto F, Arif I. Comparison between EGSnrc and MCNPX for X-ray target in 6 MV photon beam. Journal of Physics: Conference Series. 2019; 1127: 012014.

30. Allahverdi M, Zabihzadeh M, Ay MR, Mahdavi SR, Shahriari M, Mesbahi A, et al. Monte Carlo estimation of electron contamination in a 18 MV clinical photon beam. Iran. J. Radiat. Res. 2011; 9(1): 15-28.
31. Medina AL, Teijeiro A, Garcia J, Esperon J, Terron JA, Ruiz DP, et al. Characterization of electron contamination in megavoltage photon beams. Medical Physics. 2005; 32:1281-92.
32. Pelowitz DB. MCNPX Users Manual. New Mexico: Los Alamos National Laboratory; 2008.
33. Allen PD, Chaudhri MA. Photoneutron production in tissue during high energy bremsstrahlung radiotherapy. Physics in Medicine and Biology. 1988; 33:1017‑36.